Available online at www.sciencedirect.com
SCIENCE DIRECT®
Journal of Nuclear Materials 340 (2005) 93–112
journal of nuclear materials
www.elsevier.com/locate/jnucmat

Review

A review of refractory metal alloys and mechanically alloyed-oxide dispersion strengthened steels for space nuclear power systems

Mohamed S. El-Genk *, Jean-Michel Tournier

Department of Chemical and Nuclear Engineering, School of Engineering, Institute for Space and Nuclear Power Studies, The University of New Mexico, Farris Engineering Center, Room 239, Albuquerque, NM 87131-1341, USA

Received 16 June 2004; accepted 20 October 2004

Abstract

Mechanical and thermo-physical properties of refractory metal alloys and mechanically alloyed (MA)-oxide dispersion strengthened (ODS) steels are reviewed and their potential for use in space nuclear reactors is examined. Preferable refractory alloys for use in liquid metal and gas-cooled space reactors include Nb–1%Zr, PWC-11, Mo–TZM, Mo–xRe where x varies from 7% to 44.5%, T-111 and ASTAR-811C. These alloys are heavy, difficult to fabricate, and are not readily available. The advantages of the MA-ODS alloys are: (a) their strength at high temperatures (>1000 K), which decreases slower with temperature than those of niobium and molybdenum alloys; (b) relatively lightweight and less expensive; (c) low swelling and no embrittlement with exposure to high-energy neutrons (>0.1 MeV) up to 10^{27} n/m^2; and (d) high resistance to oxidation and nitration. The few data available on compatibility of MA-ODS alloys with alkali liquid metals up to 1100 K are encouraging, however, additional tests at typical temperatures (1000–1400 K) in space nuclear reactors are needed. The anisotropy of MA-ODS alloys when cold worked, and particularly rolled into tubes, should not hinder their use in space nuclear power systems, in which operation pressure is either near atmospheric or as high as 2 MPa, but joints weldability is an issue.

PACS: 81.20.E; 61.82.Bg; 81.05.Bx; 81.05.Je

Contents

* Corresponding author. Tel.: +1 505 277 5442; fax: +1 505 277 2814/5433.
E-mail address: mgenk@unm.edu (M.S. El-Genk).

0022-3115/$ - see front matter © 2004 Elsevier B.V. All rights reserved.
doi:10.1016/j.jnucmat.2004.10.118

1. Introduction

The technology development and system studies of nuclear reactor powered and electrically propelled spacecraft are being carried out under NASA's Prometheus program. This program aims at launching a nuclear powered, ion thrusters propelled spacecraft to explore Jupiter and its three icy moons (Ganymede, Callisto and Europa) sometime after 2015. Activities are being conducted to develop enabling technologies and preliminary designs of potential Space Nuclear Reactor Power Systems (SNRPSs). The basic matrix includes three energy conversion technologies and three nuclear reactor types for more than nine possible combinations. The three basic energy conversion technologies are: advanced thermo-electrics; free piston stirling engines (FPSEs); and closed brayton cycle (CBC) engines. The three nuclear reactor types are: alkali liquid metal-cooled reactors; alkali liquid metal heat pipe-cooled reactors, and He–Xe gas-cooled reactors. The fuel materials in these reactors could either be UO_2, UN or UC, with UN emerging as the preferred choice owing to its compatibility with lithium and the recent experience in its fabrication and development under the SP-100 program in the eighties and early nineties [1,2]. This fuel type has a high thermal conductivity and low swelling, but is typically clad in PWC-11 (Nb 1%Zr 0.1%C) with a thin rhenium liner to protect the cladding from potential attack by fission products [3].

Liquid alkali metals- and heat pipe-cooled space nuclear reactors could operate at temperatures ranging from 1000 K to 1500 K at near atmospheric pressure or slightly higher. The gas-cooled space reactors, however, may operate at temperatures ranging from 1100 K to 1400 K and $\geqslant$2 MPa. A key requirement is the compatibility of structure materials with nuclear fuel and alkali liquid metals and gas coolants for up to 10 years, or even longer, at typical operating temperatures. Other requirements are: long term thermal creep strength; fabricability; low ductile-to-brittle transition temperature (DBTT); good weldability and brazing; low density; low oxygen, CO_2, and nitrogen embrittlement; low irradiation swelling and embrittlement; commercial availability; well characterized mechanical and thermophysical properties; and cost.

In low-power SNRPSs, 316-stainless steel has been a suitable structure material for operating at $\leqslant$923 K, while superalloys such as Inconel 601, Haynes 25, and Hastalloy-X are good for temperatures up to 1200 K (Fig. 1). For temperatures between 1200 K and 1450 K, niobium alloys, such as Nb–1%Zr, PWC-11 (Nb–1%Zr–0.1%C), and C-103 (Nb–10%Hf–1%Ti–0.5%Zr) (Table 1) are

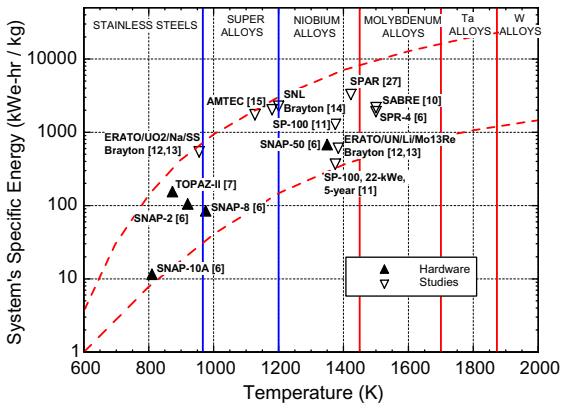

Fig. 1. Specific energy of space nuclear power systems versus reactor exit temperature.

Table 1
Nominal composition of refractory metal alloys and oxide dispersion strengthened structural materials

Alloy (Ref.)	Composition (wt%)															Melting point (K)	Recrystallization temperature (K)
	Fe	Ni	Cr	Ti	V	Mn	Zr	Nb	Mo	Hf	Ta	W	Re	Al	C	Y_2O_3	
ODS MA754 [35]	1	77.55	20	0.5	–	–	–	–	–	–	–	–	–	0.3	0.05	0.6	1673	1570
ODS MA956 [35]	74.45	–	20	0.5	–	–	–	–	–	–	–	–	–	4.5	0.05	0.5	1755	1525
ODS MA957 [36,37]	84.55	–	14	0.9	–	–	–	–	0.3	–	–	–	–	–	–	0.25	~1800	1620
ODS 1DK [38]	83.23	0.16	12.9	0.52	–	–	–	–	–	–	–	2.8	–	–	0.05	0.34	–	–
ODS 12YWT [39]	84.0	0.30	12.6	0.35	–	0.05	–	–	–	–	–	2.4	–	–	0.05	0.25	–	–
ODS 1DS [38]	85.15	0.15	11	0.4	–	–	–	–	–	–	–	2.7	–	–	0.10	0.5	–	–
ODS Eurofer97 [40]	88.91	–	8.9	–	0.2	0.45	–	–	–	–	0.14	1.0	–	–	0.10	0.3	–	–
Nb–1Zr [29]	–	–	–	–	–	–	1	99	–	–	–	–	–	–	–	–	2680	1253
PWC-11 [29]	–	–	–	–	–	–	1	98.9	–	–	–	–	–	–	0.1	–	2680	~1253
C-103 [29]	–	–	–	1	–	–	–	89	–	10	–	–	–	–	–	–	2623	1313
Mo [20]	–	–	–	–	–	–	–	–	100	–	–	–	–	–	–	–	2896	1200
TZM–Mo [29]	–	–	–	0.5	–	–	0.1	–	99.37	–	–	–	–	–	0.03	–	2893	1698
Mo–14Re [20]	–	–	–	–	–	–	–	–	86	–	–	–	14	–	–	–	2800	1645
T-111 [24]	–	–	–	–	–	–	–	–	–	2	90	8	–	–	–	–	3250	1923
ASTAR-811C [24]	–	–	–	–	–	–	–	–	–	0.7	90.27	8	1	–	0.025	–	–	–

suitable structure materials but become brittle with oxygen contamination of as little as a few parts per million [4], hence requiring surface protection and clean environment for fabrication and assembly. For up to 1700 K and as low as 1450 K, molybdenum alloys TZM (Mo–0.5%Ti–0.1%Zr) and Mo–xRe, where x varies from 7% to 44.5%, could be considered. Unlike niobium alloys, Mo–Re alloys are more resistant to oxygen embrittlement [4], but also much heavier and more difficult to machine and cold work. In addition, know-how and the large-scale production and fabrication expertise of some refractory alloys are not readily available [1,2,5].

Nuclear reactor power systems indicated in Figs. 1 and 2 have been either partially or totally developed to the hardware level (e.g., SNAP-10A, SNAP-2, SNAP-8, TOPAZ-II, SNAP-50, SPAR, and SP-100) [6–11] or based on paper studies [12–15]. In general, the higher the specific energy the higher is the operating temperature, shifting the selection of the structure material from stainless steel, at or below 923 K, to superalloys, Nb alloys, and Mo alloys above 923 K, 1200 K, and 1450 K, respectively.

Refractory alloys have high creep strength at high temperatures and excellent compatibility with alkali liquid metals as long as oxygen, nitrogen, carbon, and silicon impurities are kept below appropriate limits, typically in the range of a few to 10's ppm [16,17]. For example, Nb–1%Zr suffers embrittlement in as low as 10 ppm oxygen, which detrimentally affects its mechanical properties. Recent experiments demonstrated that oxygen embrittlement of Nb–1%Zr could occur even at oxygen concentrations as low as 5 ppm, which could also be true for other Nb alloys such as PWC-11 and C-103, pending further verification [1,4]. Other oxygen embrittlement experiments have also shown that Mo–44.5%Re retained ductility (with a measured elongation

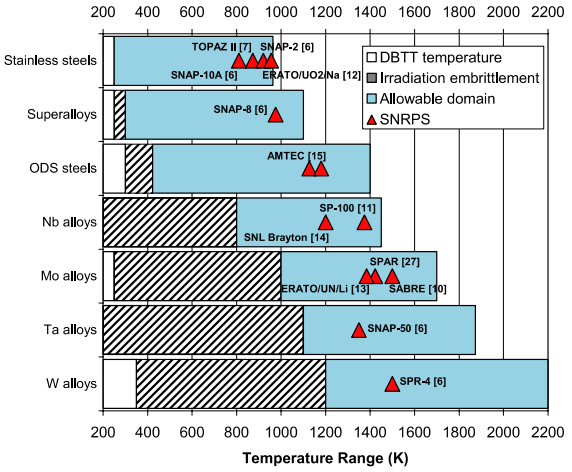

Fig. 2. Recommended operation temperature range for structural materials in space nuclear power systems.

of 19–22%), while the Nb–1%Zr specimens became brittle, with elongation <1%.

The refractory alloys are heavier than stainless steels and superalloys (8.6 g/cm^3 for Nb–1%Zr and PWC-11, 10.2 g/cm^3 for TZM, 11.9 g/cm^3 for Mo–14%Re, 16.7 g/cm^3 for T-111, and 18.4 g/cm^3 for W–4%Re) and experience irradiation embrittlement at temperatures below ~30% of their melting points (~800 K for Nb alloys, ~1000 K for Mo alloys, ~1100 K for Ta alloys, and ~1200 K for W alloys) with fast neutron's ($E >$ 0.1 MeV) fluence as low as ~10^{24} n/m^2 [1,18]. Irradiation embrittlement of the b.c.c. metals is common; it hardens the metals and is manifested in a reduction in the elongation uniformity and an increase in DBTT.

Molybdenum–rhenium alloys, developed to remedy the lack of ductility of pure molybdenum at low temperatures, and to increase creep strength [19] and the resistance to oxygen embrittlement, are stronger but much heavier than niobium alloys [4,17]. Rhenium increases the re-crystallization temperature of the Mo–Re alloy to 1450–2000 K, depending on the amount of Re (1645 K for Mo–14%Re) [20,21]. This fundamental effect of Re is pronounced with ~13 wt% rhenium. Although as much as 50 wt%Re is soluble in molybdenum, high Re content is not recommended because of the increased fabrication difficulty and the formation of the brittle sigma phase in high temperature uses [20]. Owing to the very high density of Re (21.040 g/cm^3), high temperature space nuclear power applications favor Mo–Re alloys with small Re contents ($\leqslant$14%).

A key challenge associated with using refractory alloys at present is to re-establish large-scale production capabilities and to recapture former expertise on fabricability, developing viable joints, brazing, cold work in various shapes, irradiation effects, and weldability [1,2,5]. While niobium and tantalum alloys are easier to fabricate than molybdenum alloys, they require stringent control of atmospheric impurities (including oxygen and CO_2) and are best handled in glove boxes.

Reid et al. [22] have conducted a comprehensive review of life tests of different combinations of working fluids and wall materials for use in high-temperature heat pipes, and the findings are listed in Tables 2 and 3. Oxygen embrittlement of the refractory alloy wall of the high-temperature heat pipes could be eliminated through active gettering of oxygen using zirconium or hafnium sleeves [23].

As shown in Fig. 2, refractory alloys usually suffer irradiation embrittlement at temperatures below ~30% of their melting point in fast neutron ($E > 0.1$ MeV) fluences as low as ~10^{24} n/m^2 [1,18]. Under the development programs and cooperative efforts initiated in the

Table 2
Demonstrated compatibility of key structural materials with alkali metals [6,16,22,23,27,41,42]

Material type	Temperature (K)	Alkali metal	Material/alloy	Elemental composition (w%)	MP (K)	Density (g/cm^3)
Titanium	775–875	K	Titanium	Ti	1941	4.51
Steels	875–960		304-SS	Fe–19Cr–(8–12)Ni–2Mn	1699	7.92
		Na, K, NaK,	316-SS	Fe 17.0Cr 12Ni 2.5Mo 2.0Mn 1Si 0.1C	1658	7.9
		Hg	316FR-SS	Fe 17.5Cr 12Ni 2.8Mo 1.5Mn < 0.6Si $\leqslant$ 0.02C	~1650	7.9
Superalloys	900–1150	Na, K	Inconel 750X	73Ni–15.5Cr–7Fe–2.5Ti–1Nb	1666	8.25
		Na, K, NaK	Hastelloy X	49Ni–22Cr–15.8Fe–9Mo	1523	8.2
		Na	Haynes-25	50Co–20Cr–15W–10Ni–3Fe–1.5Mn	1602	–
Niobium and its alloys	Up to 1500	Li, Na, K	Niobium	Nb	2750	8.57
		Li, Na, K, NaK	Nb–1%Zr	Nb–1Zr	2680	8.58
			PWC-11	Nb–1Zr–0.1C	2680	8.60
			C-103	Nb–10Hf–1Ti–0.5Zr	2623	8.86
Molybdenum and its alloys	Up to 1800	Li, Na	Molybdenum	Mo (brittle below ~400 K)	2896	10.28
		Li, Na, K	Mo–TZM	Mo–0.5Ti–0.1Zr	2896	10.16
		Li	Mo–44.5%Re	Mo–44.5Re	3023	13.5
Tantalum and its alloys	Up to 2200	Li, Na, K, NaK, Hg, Cs	Tantalum	Ta	3290	16.6
			T-111	Ta–8W–2Hf	3250	16.7
			ASTAR-811C	Ta–8W–1Re–0.7Hf–0.025C	–	–
Tungsten and its alloys	Up to 2200	Li	Tungsten	W (brittle below ~600 K)	3695	19.25
			W–4%Re	W–4Re	–	18.35
Carbon	Up to 3000	With thin Ta liner	Carbon	C	3923	2.25

Table 3
Life tests of alkali liquid metal heat pipes [6,22,41,43,44]

Working fluid	Material	Temperature (K)	Cumulative test time (hrs)	Reported cause of failure
Lithium	W-26Re	1875	10 000	
Lithium	TZM	1775	10 500	Weld cracking
Lithium	Nb–1Zr	1775	9000	
Lithium	Mo–13%Re	1500	11 400	
Lithium	Molybdenum	1700	25 400	Formation of large grain and lithium leakage along grain boundary
Sodium	Mo–TZM	1390	53 000	
Sodium	Molybdenum	1400	45 000	
Sodium	300-series SS	920	23 000	
Sodium	ODS MA764	1223	>5500	
Sodium	ODS MA956	1223	140	Evaporator wall perforation likely due to Al leaching
Potassium	Nb–1%Zr	1350	10 000	
Potassium	300-series SS	920	5300	
Potassium	Titanium	800	5000	
Mercury	300-series SS	600	10 000	

1980s of commercial liquid metal fast breeder reactors (LMFBRs) and fusion reactors in Japan, the European Union, and the USA however, the mechanically alloyed (MA)-oxide dispersion strengthened (ODS) steels have emerged, which could offer a better alternative as nuclear fuel cladding and structure materials and could satisfy the 1000–1400 K operating temperature range of SNRPSs (Table 1). Inconel MA-ODS754, Incoloy MA-ODS956, and Incoloy MA-ODS957 appear to be promising alternative structural materials for potential use in space nuclear reactors up to a temperature of 1373 K (1100 °C), and possibly higher. The melting point of these materials varies from 1400 °C (1673 K for Inconel MA-ODS754) to approximately 1623 °C (1800 K), depending on composition (Table 1). These materials are much stronger at high temperature than stainless steel and conventional superalloys such as Inconel 601, Haynes 25, and Hastalloy-X, while retaining the mass density advantage of these steels. Conventional superalloys can be used up to 1100 K due to their higher creep strength, however, they exhibit radiation-induced embrittlement at temperatures >773 K and fast neutron fluences $>\sim 10^{25}$ n/m^2. Therefore they can only be used in short-operation life (a few years) and lower power SNRPs at 800–1100 K. Unlike conventional superalloys, the MA-ODS steels should not have any irradiation swelling and embrittlement issues. Irradiation tests have shown this to be true up to a fast neutron ($E > 0.1$ MeV) fluence of 10^{27} n/m^2, which is slightly greater than that expected in a space nuclear reactor for 15 years operation lifetime.

This paper reviews the mechanical and thermo-physical properties of the most promising refractory metal alloys and MA-ODS steels and examines their potential for use in space nuclear reactors in the temperature range from 1000 K to 1400 K. The composition, melting point and re-crystallization temperature of the most promising alloys are given in Table 1. In this review, particular emphasis is placed on the following three MA-ODS alloys: Inconel MA-ODS754 (77.55Ni, 20Cr, 1Fe, 0.5Ti, 0.3Al, 0.05C, and $0.6Y_2O_3$), Incoloy MA-ODS956 (74.45 Fe, 20Cr, 4.5Al, 0.5Ti, 0.05C, $0.5Y_2O_3$), and Incoloy MA-ODS957 (84.55Fe, 14Cr, 0.3Mo, 0.9Ti, $0.25Y_2O_3$). The properties of these MA-ODS steels are compared with those of niobium alloys: Nb–1%Zr, PWC-11 (Nb–1%Zr–0.1%C) and molybdenum alloys: TZM, and Mo–x%Re up to 1400 K, 316 stainless steel (316-SS), and superalloys.

2. Refractory metals and alloys

For space reactors operating at temperatures >1000 K, there are several choices of refractory metals (Nb, Mo, Ta, and W) and refractory alloys. Niobium alloys (Nb–1%Zr, PWC-11, and C-103) are good up to ~1450 K, molybdenum alloys (low-carbon arc-cast molybdenum, TZM–Mo, Mo–14%Re and Mo–44.5%Re) are good up to ~1700 K, tantalum alloys (T-111, ASTAR-811C) up to ~1870 K, and tungsten alloys (W–5%Re and W–25%Re, for example) are good up to ~2200 K (Figs. 1 and 2). These service temperatures are determined based on considerations of high-temperature creep strength; fabricability; changes in mechanical properties in irradiation environment; chemical compatibility with working fluids and nuclear fuel materials (UO_2, UC or UN) [1,2]. When relevant, other properties such as static and dynamic tensile behavior; fracture toughness and weldability; and the ductile-to-brittle transition temperature (DBTT) are taken into

account as well. The upper temperature limits of the refractory alloys are generally determined by their compatibility with alkali metals and/or thermal creep rupture strength.

Refractory metals have been extensively explored for use in space nuclear reactor power applications in the SNAP and SP-100 programs in the sixties and eighties, respectively [19,24,25]. During the SNAP program in the 1960s, a number of companies were involved in the development of different niobium alloys [25]. Unfortunately, only a few of those alloys remain commercially available. Nb–1Zr was an early development and remained in use in the nuclear industry and as a general purpose high-temperature alloy. PWC-11 (Nb–1%Zr–0.1%C) was also developed in the 1960s as a higher strength alternative to Nb–1Zr but never entered commercial production. The niobium alloy C-103 (Nb–10%Hf–1%Ti–0.5%Zr) is a commercially available aerospace alloy that was developed during the Apollo program and has seen significant use in military aircraft. All three niobium alloys contain either zirconium and/or hafnium, which have been demonstrated to dramatically improve the alloys' resistance to oxygen driven alkali metal corrosion [16].

During the same time frame, tantalum alloys received significant attention and several strong alloys were developed under the sponsorship of the NASA's Lewis Research Center including T-111 (Ta–8%W–2%Hf) and ASTAR-811C (Ta–8%W–1%Re–0.7%Hf–0.025%C), which had high yield and creep strengths [24], good weldability, and demonstrated good compatibility with liquid alkali metals [16]. The development of the molybdenum alloys has been historically less energetic than that of the niobium alloys due to their difficult fabricability and poor weldability, but several promising candidates exist. Mo–TZM (Mo–0.5%Ti–0.1%Zr) is readily available and offers improved strength and ductility over the base molybdenum metal which has high DBTT ~400 K [19,20]. Recent work on the ductilization of molybdenum by the addition of rhenium has resulted in the availability of a range of molybdenum–rhenium binary alloys, with 14–44.5% rhenium [19,20].

An extensive R&D program would be required to reestablish production of PWC-11, the choice for UN fuel pins cladding in the SP-100 SNRPS, and further work is needed to develop viable joining methods for niobium structural materials [1]. Molybdenum and tantalum alloys also need significant R&D in areas such as fabrication and irradiation effects before being qualified for use in SNRPSs.

Some refractory metals and alloys also exhibit ductile-to-brittle transition temperatures above room temperature (Fig. 2), requiring particular care in fabrication and handling, and are extremely costly since they require stringent atmospheric control during fabrication. For example, molybdenum (Mo) and tungsten (W) are brittle below ~400 K and 600 K, respectively, and exhibit low fracture toughness even at temperatures above the DBTT (this is also the case for relatively pure alloys such as Mo–TZM and W–2%Re). These refractory metals can be alloyed with rhenium to decrease the DBTT and significantly increase ductility. The Nb–1%Zr alloy experiences embrittlement in as low as 10 ppm oxygen, requiring that fabrication and assembly be performed in a controlled atmosphere. The zirconium additive in this alloy reacts with the oxygen in the matrix, forming precipitates, thus decreasing embrittlement.

2.1. Operation and design stress domains of refractory metals and alloys

Fig. 3 compares the yield strengths of Mo, Nb–1Zr, PWC-11, C-103, Mo–TZM, Mo–14Re, Mo–44.5Re, and T-111. The yield strength, although not an indicator of the creep properties of the materials, it is a good measure to rank the materials in term of their strength at the operating temperatures of interest. Of note are the particularly high strengths of the molybdenum alloys Mo–14Re, Mo–44.5Re, and Mo–TZM, and of the tantalum alloy T-111 (Fig. 3). Above 1000 K, the strengths of the niobium alloys Nb–1Zr, PWC-11, and C-103 and of pure molybdenum are all comparable, but much lower than those of the Mo and Ta alloys. Based on the different densities of the strongest alloys Mo–TZM (10.16 g/cm^3), Mo–14Re (11.89 g/cm^3), Mo–44.5Re (13.5 g/cm^3), and T-111 (16.7 g/cm^3), the yield strength-to-density ratio above 1000 K favors Mo–TZM, followed by T-111 and Mo–14Re. The high strength of Mo–44.5Re is offset by the alloy's high density, because of the higher fraction of rhenium, which is heavier than tungsten in the pure form.

Figs. 4–9 present the recommended design stress domains for Nb–1Zr, molybdenum; Mo alloys TZM and

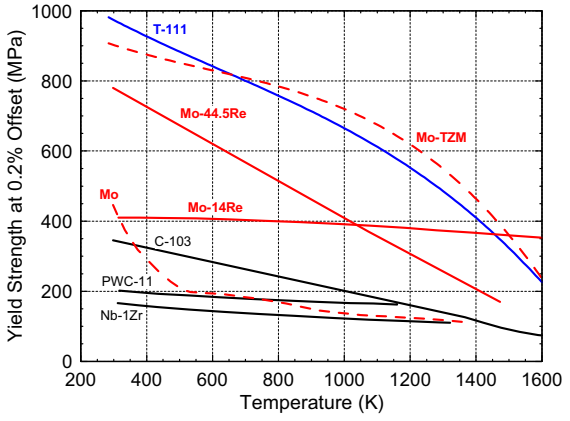

Fig. 3. Comparison of yield strengths of refractory metals and alloys [25,28–30].

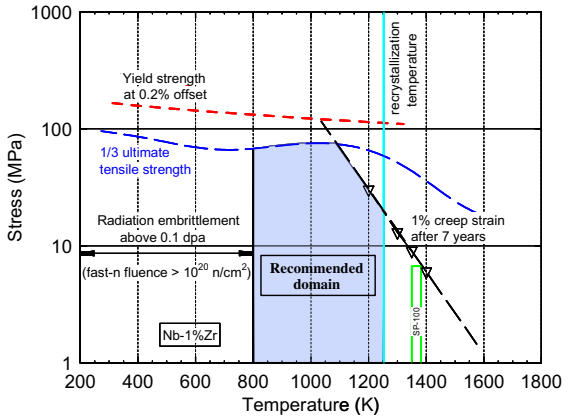

Fig. 4. Recommended design stress domain for Nb–1%Zr [25,31].

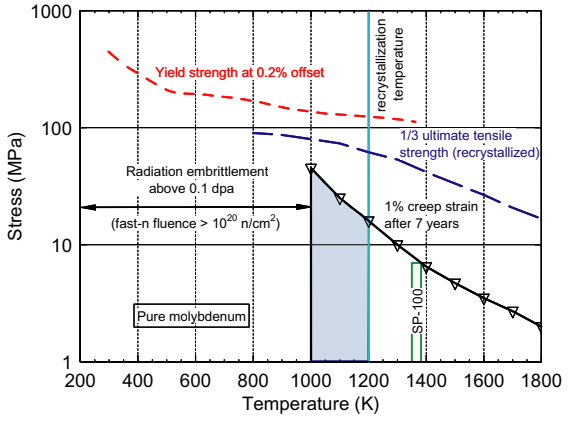

Fig. 5. Recommended design stress domain for pure molybdenum [20,28].

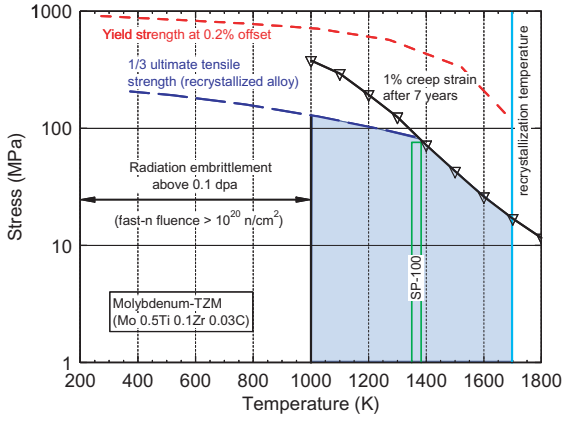

Fig. 6. Recommended design stress domain for Mo–TZM [20,29].

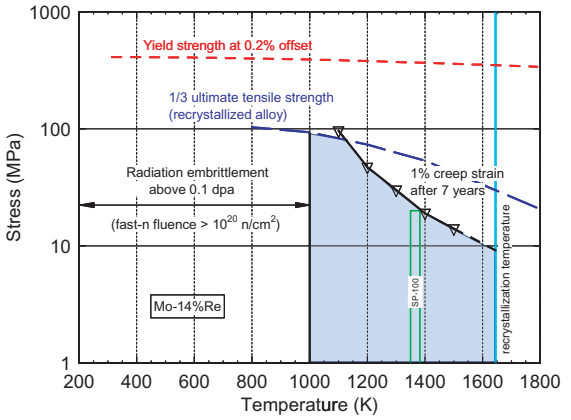

Fig. 7. Recommended design stress domain for Mo–14%Re [20,25].

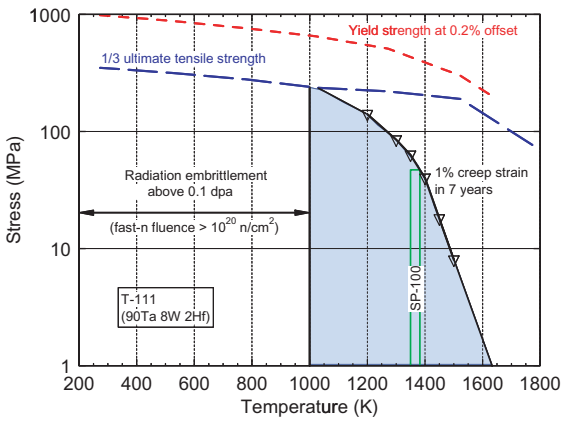

Fig. 8. Recommended design stress domain for T-111 [25,31].

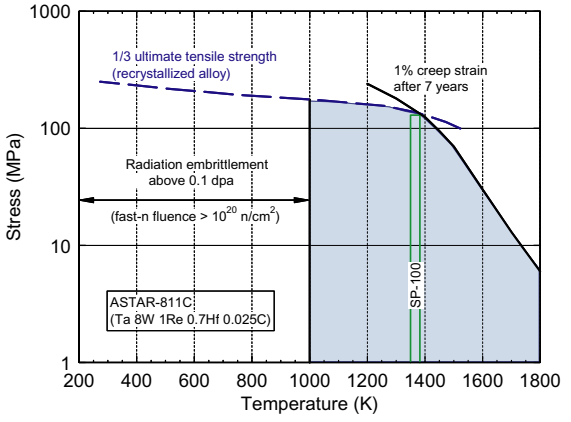

Fig. 9. Recommended design stress domain for ASTAR-811C [31,32].

Mo–14Re, and Ta alloys T-111 and ASTAR-811C. The scales are identical on all figures, for ease of comparison. A good review of the available thermal creep test data and test conditions and durations of these alloys can be found in Buckman [5]. Estimates of the radiation embrittlement, re-crystallization temperatures, and the melting points of these alloys are listed in Table 4.

Refractory alloys experience irradiation embrittlement at temperatures below typically ~30% of their melting points (~800 K for Nb alloys, ~1000 K for Mo alloys, ~1100 K for Ta alloys, and ~1200 K for W alloys) with fast neutron's ($E > 0.1$ MeV) fluence as low as $\sim 10^{24}$ n/m^2 [1,18]. Irradiation embrittlement of the b.c.c. metals is common; it hardens the metals and is manifested in a reduction in the elongation uniformity and an increase in DBTT. Irradiation embrittlement does not become an issue until the SNRPS has been placed safely into orbit and the startup of the nuclear reactor is initiated. The startup should be performed as fast as possible to raise the temperature quickly and minimize the exposure time of the cold refractory structural material (<0.02 dpa) to neutron irradiation. Similarly, in case a reduction in the nuclear reactor's power is needed, the operation temperature should be kept well above the irradiation embrittlement limit of the refractory alloy structure.

Space nuclear reactor's structural materials should also be operated below their re-crystallization temperature, since the tensile strength and ductility of the non-re-crystallized alloys are generally higher than those of re-crystallized ones, by as much as a factor of two in some cases. However, it is worth noting that because of different deformation mechanisms, the tensile strength and ductility values derived from tensile tests are not a good predictor of the temperature creep properties of the structural materials. While the creep properties of unre-crystallized alloys may be better, other metallurgical factors, such as the grain size, can strongly affect the creep strength. For example, a re-crystallized microstructure with a large grain size has better creep resistance than a fine grain, fully re-crystallized microstructure. In an unre-crystallized microstructure, the high dislocations density and interfacial area due to subgrains, which increase the vacancy diffusion and the dislocation climb, result in high creep rates. In addition, an unre-crystallized microstructure can often retain textures from the fabrication steps, which may result in banding of the grain sizes and the formation of elongated grains, resulting in anisotropic strength properties.

During annealing, a work-hardened material is exposed to a sufficiently high temperature for a period long enough to cause full re-crystallization of the grain structure, removing all residual stresses and softening the material, but it also reduces its strength. As shown in Figs. 4 and 5, and Table 2, pure molybdenum and niobium alloys (Nb–1Zr, PWC-11, and C-103) have relatively low re-crystallization temperatures, in the range 1200–1313 K.

The rectangular box labeled SP-100 in Figs. 4–9, indicating the operating temperature for the SP-100 space

Table 4
Thermo-physical properties of key structure materials for space nuclear reactor power systems

Property	MA754 [35,56]	MA956 [35,56]	MA957 [36]	Nb–1%Zr [19,20,25,31,57]	Mo–14%Re [19,20,25,31]
Room temperature density (g/cm^3)	8.3	7.25	~7.3	8.58	11.89
Melting point (K)	1673	1755	1800	2680	2800
Recrystallization temperature (K)	1570	1525	1620	1253	1645
DBTT (K)	–	273–373	200–330	~150	73 (cold worked) 150 (re-crystallized)
Radiation embrittlement (K)	–	~450	~400	~800	~1000
Properties at 1373 K (1100 °C)					
Thermal conductivity (W/m K)	34.2	27.0	–	62.3	68[a]
Specific heat (J/kg K)	720	769	–	352	296
Thermal diffusivity (m^2/s)	5.72×10^{-6}	4.84×10^{-6}	–	20.6×10^{-6}	19.3×10^{-6}
CTE (K^{-1})	17.4×10^{-6}[a]	15.5×10^{-6}	21×10^{-6}[a]	$\sim 8 \times 10^{-6}$	$<8 \times 10^{-6}$
Yield strength (MPa)	165 (uniaxial)	85 (uniaxial)	10[a] (hoop)	103	370
1/3 ultimate tensile strength (MPa)	56 (uniaxial)	30 (uniaxial)	10[a] (hoop)	39	55
1/3 creep rupture after 10^4 h (MPa)	27 (uniaxial)	15.3 (uniaxial)	–	–	–
2/3 creep rupture after 10^5 h (MPa)	–	–	3[a] (hoop)	–	–
1% creep after seven years (MPa)	–	–	–	7[a]	20

[a] Extrapolated.

nuclear reactor power system (1350–1383 K) [11], is shown only for reference. As shown in Fig. 6, the recommended design stress domain for Mo–TZM is bounded on top by 1/3 the ultimate tensile strength up to about 1373 K, and by the stress to cause 1% creep strain after 7 years above 1373 K. On the left and right, radiation embrittlement (~1000 K) and re-crystallization (1698 K) temperatures bound the design stress domain, respectively.

The Mo–14%Re refractory alloy exhibits a similar design stress domain than Mo–TZM, except that the upper bound stress levels are about three times lower than those of Mo–TZM. Also, the re-crystallization temperature of Mo–14%Re is 53 K lower than that of Mo–TZM (Table 1, Figs. 6 and 7). The design stress domain of the tantalum alloy T-111 is bounded on the left by irradiation embrittlement (below ~1000 K) and on top and on the right by the stress to cause 1% creep strain after seven years (Fig. 8). While the allowable stress for T-111 is higher than that of Mo–14%Re up to ~1450 K, it subsequently drops precipitously to almost zero at ~1650 K, while that of Mo–14%Re decreases steadily to as much as 10 MPa at 1645 K, which is the re-crystallization temperature of Mo–14%Re. By contrast, the re-crystallization temperature of T-111 is >1900 K (Table 1) and is not a concern for the temperature range of interest in space nuclear reactors, 1000–1600 K. This difference in behavior between these alloys is also exhibited in the yield strength shown in Fig. 3. The precipitous drop in the stress to cause 1% creep strain after seven years for T-111 may be an indicator of aging embrittlement, which has been observed at 1100–1500 K after 1000–5000 h [26]. The combination of tungsten and hafnium or zirconium found in the commercial alloys T-111 and Cb-752 can lead to aging embrittlement and increases the susceptibility of ternary and more complex alloys to hydrogen embrittlement [26]. Modification of the alloy composition helps eliminate this embrittlement caused by the segregation of Hf and Zr to the grain boundaries, which typically occurs in the temperature range between 0.35 and 0.47 times the melting point.

As shown in Fig. 9, the tantalum alloy ASTAR-811C is the strongest of all the refractory alloys. The ultimate tensile strength of the re-crystallized alloy is still very high, comparable to that of the unre-crystallized T-111 and higher than that of Mo–TZM. The stress to cause 1% creep strain after seven years at 1650 K in ASTAR-811C is ~20 MPa, compared to 21 MPa for Mo–TZM and 10 MPa for Mo–14%Re.

2.2. Oxygen embrittlement in niobium refractory metal alloys

Experiments performed at Oak Ridge National Laboratory have demonstrated that when Nb–1%Zr was heated to elevated temperature (1198 K) in inert atmosphere containing small concentrations of oxygen (1–5 ppm), its mechanical properties were detrimentally affected [4]. Also, the Nb–1%Zr coupons gained weight and increased in thickness with time due to the gettering of oxygen by the zirconium. After heat treatment at 1198 K for 150 h, the tensile specimen developed <1% elongation at room temperature, compared to 25% elongation for as-received, untreated specimens [4]. Tensile specimens heat treated at 1198 K for up to 3015 h in vacuum developed 20–23% elongation at room temperature. These results demonstrated that oxygen embrittlement of Nb–1%Zr could occur even at oxygen concentrations as low as 5 ppm, which could also be true for other Nb alloys such as PWC-11 and C-103, pending further verification [1,17].

Oxygen embrittlement experiments were also performed using Mo–44.5%Re sheets (~0.5 mm thick) [4,21]. Measurements of room temperature mechanical properties showed that the Mo–44.5% specimen retained ductility (with a measured elongation of 19–22%), while the Nb–1%Zr specimens became brittle, with elongation <1% [4].

2.3. Increase in ductility by rhenium alloying

Molybdenum–rhenium alloys, developed to remedy the lack of ductility of pure molybdenum at low temperatures, and to increase creep strength (Figs. 5 and 7, [19]) and the resistance to oxygen embrittlement, are stronger but much heavier than niobium alloys [4,17]. Commercially pure Mo lacks toughness when re-crystallized (complete re-crystallization occurs in 1 h at 1200 K). Low carbon arc-cast (LCAC) molybdenum has a DBTT of 340 K when re-crystallized, but with the addition of 14 wt% rhenium the DBTT decreases to 150 K [20,21] in the re-crystallized condition. The hardness of Mo–41%Re is about 60% higher than unalloyed molybdenum since Re increases the re-crystallization temperature of the alloy to 1450–2000 K, depending on the amount of Re (1645 K for Mo–14%Re) [20,21]. This fundamental effect of Re is pronounced with ~13 wt% rhenium. Although as much as 50 wt%Re is soluble in molybdenum, high Re content is not recommended because of the increased fabrication difficulty and the formation of the brittle sigma phase in high temperature uses [20]. Owing to the very high density of Re (21.04 g/cm^3), high temperature space nuclear power applications favor Mo–Re alloys with small Re contents (⩽14%). The thermal conductivity of the Mo–Re alloys decreases with increasing rhenium content and the coefficient of thermal expansion (CTE) increases with increasing Re up to 30 wt%. With higher Re content, the CTE of Mo–Re alloys exceeds that of TZM and pure molybdenum [20].

Another advantage of using Mo–Re alloys in fast-spectrum space nuclear reactors stems from the fact that rhenium is an acceptable spectral-shift absorber material. Rhenium has a relatively low neutrons absorption cross-section at epithermal and fast neutrons energies, but a much higher cross-section at thermal energies. In the event of a launch accident where the reactor would fall in water or wet sand, the increase in reactors reactivity due to the spectral shift would be partly compensated by the increased neutrons absorption in the refractory structural material [33,34].

2.4. Compatibility of refractory alloys with alkali metals

A corrosion mechanism of refractory alloys in alkali metals is the transport of the structural material by dissolution in the hot zones, and deposition in the colder zones. Other mechanisms are reactions with impurities, particularly non-metallic contaminants such as oxygen, carbon, nitrogen, and silicon [17,22]. Corrosive failures could also result from the reaction of trace impurities with the structural materials to form mobile compounds, which are soluble in alkali metal working fluids. Many of these corrosion mechanisms could be alleviated by the proper selection of structural materials and the working fluid, ensuring their high purity, and using appropriate cleaning and filling techniques during fabrication and loading of the working fluid.

A life test involving a short (2 m long) lithium heat pipe fabricated from low-carbon, arc-cast Mo has been performed for 25 400 h at 1700 K with a thermal power transport of ~1 kW [27]. This heat pipe experienced extensive grain growth to the point that the average grain diameter was several times larger than the 1.0 mm thick wall. The lithium working fluid leaked out when the heat pipe was fastened into a lathe to re-machine the support system [27].

Tests conducted during the SPAR and SP-100 programs [6,16,27] demonstrated good compatibility of refractory metals with alkali metals, provided that the oxygen content is kept very low, less than 1–10 ppm [17,22]. Niobium and tantalum are particularly susceptible to oxygen driven attacks, even in Na containing <1–10 ppm O_2. Using refractory alloys containing traces of oxygen getters such as Zr or Hf alleviates this concern. Examples are the niobium alloys: Nb–1%Zr, PWC-11, and C-103, and the tantalum alloys T-111 and ASTAR-811C (Table 1). Pure molybdenum and tungsten do not appear to be as susceptible to oxygen-assisted alkali metal attack, like tantalum and niobium, and non-gettered Mo and W alloys have demonstrated acceptable compatibility with alkali metals in capsule tests [19]. Pure molybdenum and tungsten, however, suffer from high DBTT temperatures (W more so than Mo). This concern has been addressed by alloying these metals with other refractory metals, such as Mo–TZM and Mo–Re, which offer improved strength and ductility over pure Mo. The Mo–13Re alloy has excellent high-temperature creep strength, low-temperature ductility for launch conditions and excellent compatibility with lithium (>11 000 h testing at 1500 K, Table 2) and UO_2 fuel [6]. Similarly, Mo–TZM and Na have excellent compatibility (tested for 53 000 h at 1390 K, Table 2).

2.5. Fabricability and weldability of refractory metals and alloys

Niobium alloys offer the advantage of easy fabricability, high ductility, high melting temperature, low DBTT and relatively low density. However, as mentioned earlier, the strength of these alloys is relatively low, and their resistance to oxidation at elevated temperature is extremely poor, requiring fabrication and handling in inert-gas glove boxes and welding in vacuum chamber. Commercial Nb–1Zr has been very well characterized in the literature, however it has only moderate strength at high temperature (Fig. 4), and performs well only in the temperature range where advanced nickel-based superalloys can be successfully used as well. Nb–1Zr also has a very low re-crystallization temperature (1253 K). The PWC-11 alloy that is three times stronger in the SP-100 temperature range of interest (1400–1600 K), was developed by adding 0.1% carbon to promote the formation of very fine carbide precipitates for strengthening [45]; however, it does not have an extensive manufacturing and property database [46]. Recent attempts to reproduce this alloy on a commercial scale have failed, possibly due to a combination of factors such as processing history and the increased purity of today's niobium versus that used in the 1960s program [2]. For probably the same reasons, Nb–1Zr material produced in the 1980s has lower creep strength than the specimen produced in the 1960s [5]. Therefore, an extensive R&D program would be required to re-establish production of PWC-11, and further work is needed to develop viable joining methods of the Nb structural alloys. The alternative cladding and structural materials (Mo and Ta alloys), discussed next, need also significant R&D in the areas of fabrication and radiation effects before qualified for use in SNRPSs [1].

Tantalum alloys have much higher strength, but also higher neutron cross-section, higher density and decreased weldability compared to niobium alloys [2]. The higher density of Ta alloys (nearly twice that of the Nb alloys) reduces somewhat their advantage of strength since thicker Nb alloy components could be used for nearly the same weight penalty. For space, liquid alkali metal-cooled reactors, fabrication and handling of the Ta alloys require the same care and

attention to oxygen contamination and are more expensive than Nb alloys.

ASTAR-811C (Fig. 9) derives its strength from both solid solution and dispersed-phase strengthening. One potential drawback is that its mechanical properties are highly affected by processing, so that fabrication must be controlled precisely. The strong T-111 and ASTAR-811C have in the past been produced as commercially sized products. During the 1960s, ~1,950 kg of final T-111 product ranging from 0.13-mm thick foil to wire, sheet, plate, tubing and pipe were produced commercially to fabricate test components for simulated Rankine cycle tests up to 10 000 h [5]. These T-111 materials in the re-crystallized form have a bend DBTT near liquid nitrogen temperature, which does not change significantly after gas tungsten-arc (GTA) welding, even after exposure for times up to 5000 h at 1423 K.

As mentioned earlier, pure molybdenum, like tungsten (but to a lesser extent), suffers from lack of ductility well above room temperature after welding or any operation resulting in re-crystallization. Alloying of molybdenum with rhenium improves fabricability, but an addition of more than 43 at.% Re is normally considered necessary to significantly improve fabricability [2,30]. Researchers at the NASA's Lewis Research Center prepared 5.08 cm-diameter ingots of Mo–14%Re by electron beam melting and conducted creep rupture tests on sheet and rod. They reported that the alloy was ductile at room temperature, however brittle cleavage fracturing was observed on as-welded specimen [5]. Recently, arc-melted Mo–41%Re has been produced at the Oak Ridge National Laboratory using a manufacturing process similar to that used for the production of the iridium alloy for the encapsulation of plutonium dioxide in the General Purpose Heat Source [47]. Initial tests indicated that Mo–41%Re could be electron-beam welded without the porosity normally observed in welded powder metallurgy products; the welds exhibited good ductility [47].

Mo–Re alloys are attractive for space nuclear power systems from the point of views of good compatibility with nuclear fuels and liquid alkali metals, and their much stronger resistance to oxidation than Nb and Ta alloys. For example, Mo–Re alloys can be welded to tungsten in Inert Gas (TIG) rather than in vacuum for the Nb and Ta alloys, a much simpler proposition. However, the fabrication of Mo–Re alloys is difficult and complex, and no large parts of Mo–Re are currently made [2]. Molybdenum alloys only maintain their strength in wrought form, and re-crystallization during processing would limit their effectiveness. Therefore, these alloys are considered high risk due to the lack of confidence that they could maintain both strength and ductility in the post-welded form [48]. To date, no commercial size product of Mo–13Re or Mo–14Re alloys has been produced. The composition range for this alloy has not been firmly established by specification, nor have the properties of various product forms been determined [5].

3. Mechanically alloyed oxide dispersion strengthened alloys

MA-ODS754 has a density of 8.3 g/cm^3 and MA-ODS956 and Incoloy MA-ODS957 have a density of 7.3 g/cm^3. The melting points of MA-ODS754, MA-ODS956, and MA-ODS957 are 1400 °C (1673 K), 1482 °C (1755 K) and ~1623 °C (1800 K), respectively (Table 1, [35–37]). ODS steels with high strength at elevated temperatures have been developed for more than a decade in Europe, USA, Japan, and Russia. Oxide additives of interest have been titania (Ti_2O_3) and yttria (Y_2O_3). Commercial manufacturing involves mechanical alloying of rapidly solidified alloy and ultra fine oxide powder [35,49] followed by consolidation by hot extrusion, rolling or hot isostatic pressing (HIPping). The principal function of the oxide additives is to retard re-crystallization after cold or hot working. The dispersed fine Y_2O_3 (and Y–O–Ti) oxide particles improve high-temperature strength by blocking mobile dislocations and reducing irradiation swelling (0.5% per 100 dpa ion irradiation and 1–2% per 100 dpa electron irradiation of ODS-13Cr ferritic steel; [50]) by acting as trapping sites for point defects induced by radiation displacement. The addition of a small amount of Ti further reduces the oxide particles size to 3 nm [38–51], significantly improving the creep rupture strength. It is believed that during mechanical alloying, yttria decomposes and dissolves in the metal matrix. Following annealing at >1373 K, extremely fine and stable Y–Ti–O oxides precipitate in the matrix (α-Y_2TiO_5). Typically yttria ODS steels are superior to TiO_2 ODS steels. The addition of TiO_2 during the MA process is not as effective in distributing the fine oxide particles in the ferritic matrix as Ti [38]. Titanium tends to segregate at the grain boundaries and promotes χ-phase transformation at temperature >1073 K [50], both of which are detrimental to the strength and ductility of the ODS alloys. With aluminum additive, the resulting nano-size oxide particles change to the chemical form $2Y_2O_3$–Al_2O_3, while retaining their original size [38]. However, alumina particles are expected to increase in size upon heating, therefore, are less effective in retarding or preventing re-crystallization.

Recent tests of sodium heat pipes with Inconel MA-ODS754 and Incoloy MA-ODS956 walls were conducted at LANL [43]. These heat pipes were tested at 1223 K for ~43 h at LANL before they were delivered to Knolls Atomic for life testing [44]. Test results so far have shown that the sodium/MA-ODS754 heat pipe

continued to operate normally after 5500 h at 1223 K and evaporator radial heat flux of 18 W/cm^2, while the sodium/MA-ODS956 heat pipe failed after only 140 h of operation, due to the perforation of the evaporator wall, attributed in part to the presence of aluminum as an alloy constituent [44]. For space nuclear reactors cooled by a gas mixture of He and Xe at reactor temperatures $\leqslant$1400 K, the MA-ODS alloys (or steels) are particularly very attractive as structure materials.

The strength anisotropy of the two ferritic MA-ODS alloys when rolled, lowering their hoop strength, would not be an issue with alkali liquid metal heat pipes, alkali liquid metal, or gas-cooled space nuclear reactors operating at up to 4 MPa (~40 atm) and <1400 K. Results of ongoing research in the USA, Japan, and Europe, suggest that such strength anisotropy could be eliminated using special thermal treatments [38,51,52]. Reported results have been very promising [52], but are yet to be transferred to the manufacturing sector. MA ODS alloys are less expensive than refractory alloys. Both MA-ODS754 and MA-ODS956 are commercially available for a host of high temperature industrial applications. However, MA-ODS957 is not currently produced commercially, but could be fabricated by Special Metals Corporation on a special order. Table 4 compares the properties of these MA-ODS alloys with those of Nb–1%Zr and Mo–13%Re refractory alloys.

Fig. 10 shows that the yield strengths of the ODS alloys (MA-ODS754, MA-ODS956, and ORNL 12YWT: 84%Fe, 0.3%Ni, 12.6%Cr, 0.35%Ti, 0.05%Mn, 2.4%W, 0.05%C, 0.25%Y_2O_3), nickel superalloy and high-chromium ferritic/martensitic steels are much higher than that of 316-FR-SS up to ~900 K, then drop precipitously in the temperature range of 950–1150 K. Although the yield strength of the MA-ODS alloys decreases in this temperature range, their strength is greater than or equal to that of the niobium alloys Nb–1%Zr, PWC-11, and C-103 up to ~1400 K. The Mo–TZM, Mo–14%Re, and T-111 alloys maintain higher strength to temperatures >1600 K (Fig. 10), at the expense of higher mass density (Table 2). The MA-ODS956 and MA-ODS957 are ferritic alloys with the following composition by weight: 13–20%Cr, 0.2–1.5%Ti, <1%Mo, <1%yttria (Y_2O_3), and Fe balance [49]. MA-ODS956 is the first alloy to be manufactured commercially, while the MA-ODS957, a similar alloy but with lower Cr content and no Al, has been developed for enhanced radiation damage resistance. The Cr increases strength and oxidation resistance and stabilizes the ferritic structure at elevated temperatures. The small additions of Mo and Ti improve the ductility and oxidation resistance of the alloy [49]. These metals are believed to combine with trace impurities of N and C present in the alloy to form carbides and nitrides within the metal matrix, thus preventing grain boundary embrittlement caused by chromium carbide or nitride formation. In addition, Ti additive in excess of 0.2 wt% prevents Cr volatilization during annealing. The presence of Al up to 5 wt% (nominally 4.5 wt%) in MA-ODS956 strongly increases oxidation resistance because it forms alumina scale [53,54]. On the other hand, the alumina scale may be vulnerable to attack by liquid Na [44,49], thus should be limited to <1 wt% and C should be kept <0.1 wt% in ODS alloys used with liquid metals such as Na or Li. In general, the DBTT of MA-ODS steels increases with the addition of the oxide dispersion phase. Mechanical alloying, however, is vulnerable to impurity contamination, and alumina stringers are introduced as impurities in the ferrochrome powder source of the master alloy. Therefore, extremely low carbon and alumina contents are key to the use of ODS alloys in liquid metal-cooled reactors and in liquid metal heat pipes.

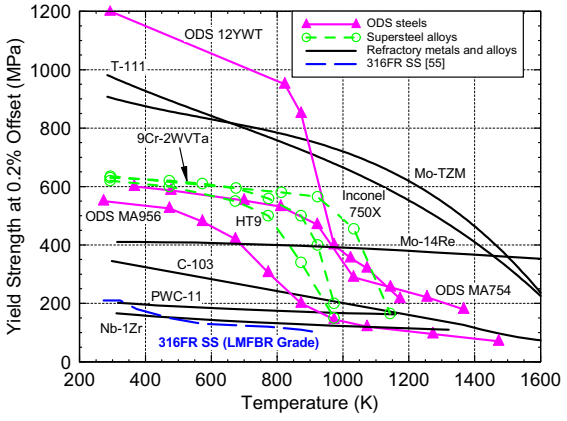

Fig. 10. Comparison of the yield strengths of key materials for space nuclear reactors [55,58,59].

3.1. Operation and design stress domains of MA-ODS alloys

Figs. 11–13 present the recommended design stress domains for MA-ODS754, MA-ODS956, and MA-ODS957, respectively. Estimates of radiation embrittlement and re-crystallization temperatures and the melting points of these alloys are listed in Table 4 and delineated in these figures. The rectangular box labeled SP-100 indicates the operating temperature for the SP-100 space nuclear reactor power system (1350–1383 K) [11]. As shown in Fig. 11, the recommended design stress domain for MA-ODS754 is bounded on top by 1/3 the ultimate tensile strength up to about 1000 K, and by 1/3 the creep rupture strength (after 10^4 h) above 1000 K. On the left and right, radiation embrittlement and re-crystallization temperatures bound the design stress domain, respectively. As indicated in Fig. 11, MA-ODS754 exhibits high strength (as high as Mo–14%Re) up to its re-crys-

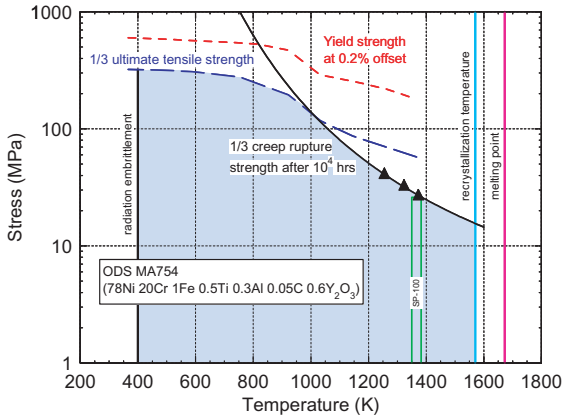

Fig. 11. Recommended design stress domain for MA-ODS754 [35,56].

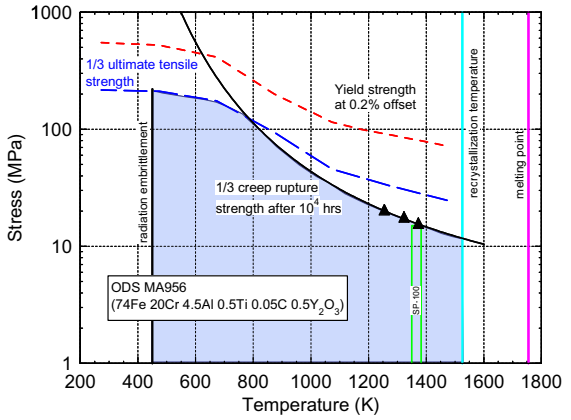

Fig. 12. Recommended design stress domain for MA-ODS956 [35,56].

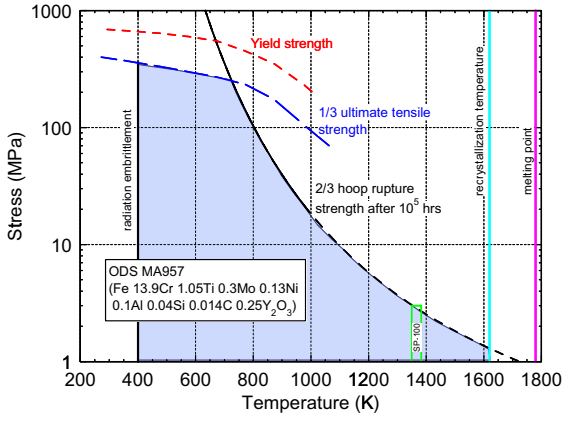

Fig. 13. Recommended design stress domain for MA-ODS957 [36].

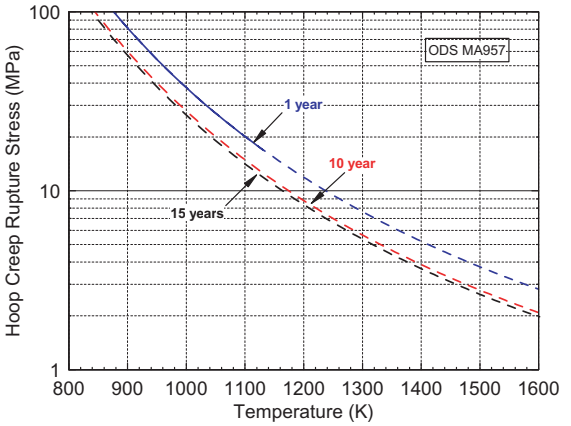

Fig. 14. Hoop rupture strength for Incoloy MA-ODS957 [36].

tallization temperature of 1570 K, which is only about 100 K below its melting point.

MA-ODS956 is nearly as strong as MA-ODS754, except that its re-crystallization temperature is 45 K lower (Fig. 12, Table 4). Below 750 K, the recommended design stress domain for MA-ODS957 is bound by 1/3 of its ultimate tensile stress and above 750 K by 2/3 of its rupture strength after 10^5 h. The values of the hoop rupture strength of MA-ODS957 (black dashed line) in Fig. 13 are extrapolated using a Larson–Miller correlation developed based on creep rupture experimental data in the temperature range 923–1123 K and rupture times up to 25 000 h [36]. The effect of temperature on the hoop rupture strength of MA-ODS957 steel for 1, 10, and 15 years operation is delineated in Fig. 14. As this figure indicates, the hoop rupture strength decreases almost exponentially with increasing temperature, but the rate of decrease becomes progressively lower with temperatures above ~1250 K. At 1400 K, increasing the service (or operation) time from one to 10 years reduces the hoop rupture strength by only ~20%, and by an additional 10% after 15 years. The inherent anisotropy in the mechanical properties of the MA-ODS alloys when rolled into tubes is discussed next.

3.2. Strength anisotropy of MA-ODS alloys

Japan Nuclear Cycle Development Institute (JNC) has been a leading organization in the development of MA-ODS steels, with its current emphases on mass production processing, joining, inspection, and developing irradiation and engineering database to qualify these alloys for use in commercial liquid metal-cooled fast reactors by the year 2015 [51]. Research results have shown that MA-ODS cladding tubes manufactured by hot-extrusion and warm-rolling processes exhibit degradations in both the creep rupture strength and ductility

in the biaxial hoop direction. Since the hoop rupture strength would limit the primary stress mode in fission gas-pressurized fuel pins, the fabrication of equiaxed grains along with the increase of the biaxial creep strength and ductility of MA-ODS steels for cladding have been critical development issues. The strength anisotropy of rolled ODS alloys has been attributed to sliding at the grain boundary of extremely elongated, bamboo-like grains (with an aspect ratio of 10–50) in the longitudinal direction [51]. Extruded and rolled ODS steels generally have a very fine grain size (<1 μm). A large columnar structure is usually obtained by zone annealing, which also produces a strong texture due to secondary re-crystallization (also referred to as exaggerated grain growth). In order to soften the materials hardened in extrusion and rolling and suppress strength degradation, the grain morphology must be controlled. Since 1995, two different heat treatment techniques for manufacturing ODS steel tubing with equiaxed and homogeneous grains have been investigated:

(a) Re-crystallization of MA-ODS ferritic steel with 12 wt%Cr (corrosion resistant alloys) by adequate heat treatments following the cold rolling manufacturing of the cladding tubes [52].
(b) Transformation of the ferritic–martensitic α-phase MA-ODS ferritic steel with 0.1–2 wt%C and 9–11 wt%Cr (radiation embrittlement resistant alloy) into austenitic γ-phase at a heating rate of 0.083 K/s from 1157 K to 1233 K [38,51].

Fig. 15 compares the creep rupture strengths in the hoop and uniaxial directions of uncrystallized 1DK ODS ferritic cladding tube and a re-crystallized specimen [52]. The hoop rupture strength of the 1DK ODS ferritic steel (83.23%Fe, 12.9%Cr, 2.8%W, 0.52%Ti, 0.16%Ni, 0.05%C and 0.34%Y_2O_3) is ~2.5 times lower than its uniaxial strength (Fig. 15). This strength anisotropy completely disappears in re-crystallized ODS ferritic steel tube (Fig. 15). Even though a re-crystallized ODS steel has lower uniaxial strength than uncrystallized steel, its hoop strength is ~40% higher.

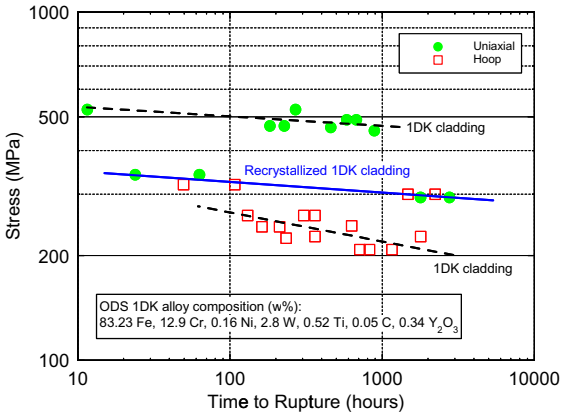

Fig. 15. Comparison of creep rupture strength of uncrystallized and re-crystallized 1DK ODS ferritic cladding tubes at 973 K [52].

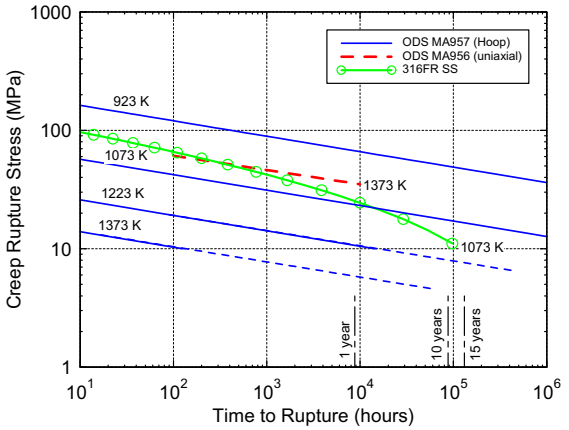

Fig. 16. Comparison of Hoop rupture strength of MA-ODS957 with uniaxial rupture strength of MA-ODS956 and 316FR-SS [35,36,56].

Hot isostatic pressing (HIPping), which is regarded as the most promising production route for nearly end shaped structures, does not induce strength anisotropy in the material. The Eurofer97 ODS alloy (Table 1), an ODS ferritic/martensitic steel with the composition: 89.33%Fe, 8.9%Cr, 1.1%W, 0.47%Mn, 0.2%V, 0.14%Ta, 0.11%C, and 0.3%Y_2O_3, when prepared by HIPping showed no identifiable difference in transverse and longitudinal cuts [40].

Fig. 16 compares the hoop rupture strength of the MA-ODS957 with those of the MA-ODS956 (in the uniaxial direction) and 316FR-SS. At 1073 K, the hoop strength of the MA-ODS957 tubing is higher than the creep rupture strength of 316FR-SS for rupture times more than 10 000 h. At 1373 K, representative of the SP-100 space nuclear reactor power system [11], the hoop rupture strength of MA-ODS957 is about a factor of 6 lower than the uniaxial rupture strength of MA-ODS956 for 1 and 15 years (Fig. 16). Nonetheless, the extrapolated rupture data at 1373 K suggests that MA-ODS957 steel could retain a hoop rupture stress of 4 MPa after 15 years, which is more than adequate for most space nuclear reactor power system applications.

Fig. 17 compares the recommended maximum operation and design stress for the MA-ODS alloys with those for 316-FR-SS and selected refractory metal alloys. As this figure indicates, the MA-ODS754 uniaxial strength at temperatures up to its re-crystallization (1570 K) is greater than those for Nb–1%Zr and Mo–14%Re. The hoop rupture strength of MA-

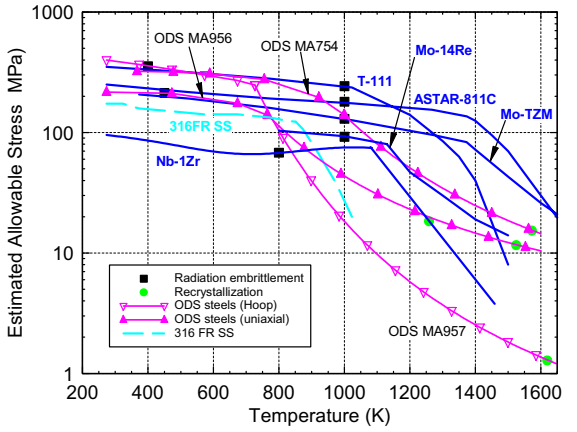

Fig. 17. Comparison of allowable stress for MA-ODS steels, 316-FR-SS, and refractory alloys.

ODS957 tubing is lower than that of Nb–1%Zr above 850 K, but is as much as 50% of this refractory alloy's strength at ~1450 K. The re-crystallization temperature of MA-ODS754 (1570 K) is close to that of Mo–14%Re (1645 K). The lower uniaxial strength of Incoloy MA-ODS956 is higher than that of Nb–1%Zr at >1250 K (Fig. 17). Such temperature is close to the re-crystallization temperature of Nb–1%Zr. The current state of knowledge on the irradiation resistance of MA-ODS steels is reviewed and discussed next.

3.3. Irradiation embrittlement of MA-ODS alloys

Since mid-1980s, materials programs in Japan, European Union, and USA have focused on developing *reduced-activation* ferritic/martensitic steels for fusion reactors. The average neutron energy in fusion reactors (~14 MeV) is much higher than in fission fast reactors (<1 MeV), thus the reported data on irradiation effects on MA-ODS steels for fusion applications are more than applicable to their use in space nuclear power systems. The ODS alloy Fe–14Cr–1Ti–0.3Y_2O_3 when irradiated with 4-MeV Ni ions up to 150 dpa at 723 K and 923 K experienced essentially no swelling, <0.1 vol.% [60]. The dispersed Y_2O_3 (and Y–O–Ti) fine oxide particles in MA-ODS steels improve their high-temperature strength by blocking mobile dislocations, thus reducing irradiation swelling (0.5% per 100 dpa ion irradiation and 1–2% per 100 dpa electron irradiation for MA-ODS 13Cr ferritic steel) by acting as trapping sites for point defects induced by radiation displacement [50]. Reported results confirmed that MA-ODS steels should not have any irradiation swelling or embrittlement concerns due to exposure to high-energy neutrons up to a fast neutron ($E > 0.1$ MeV) fluence of 10^{27} n/m^2. Such neutron fluence is higher than that expected in space nuclear reactors during 10–15 years operation lifetime.

Recently reported test results [61] for MA-ODS956 and MA-ODS957 at 420 °C (693 K) and 205 dpa, which corresponds to a fast neutron fluence ($E > 0.1$ MeV) of $6.4–9.7 \times 10^{27}$ n/m^2, showed swelling remained below 1.8%. No evidence of subgrain structure has been identified in MA-ODS956, but extensive void development (up to 4 vol.%) occurred in MA-ODS957 in regions where re-crystallization had occurred prior to irradiation. When properly manufactured with uniform oxide dispersoid in the subgrain structure, the ODS alloys remained radiation damage free to doses as high as 205 dpa [61]. These test results confirmed the high swelling resistance and microstructure stability of MA-ODS ferritic steels.

3.4. Oxidation and nitration resistance of MA-ODS alloys

MA-ODS754 and MA-ODS956 are commercially produced in large quantities and used in a host of high temperature industrial applications. MA-ODS956 offers the best combination of high-temperature strength and oxidation resistance; MA-ODS957 has similar characteristics and although not currently produced commercially, could be fabricated on a special order. MA-ODS754 has extremely high corrosion resistance due to its nickel–chromium matrix. In addition, the yttria dispersoids in this alloy result in exceptional high-temperature strength and creep resistance. MA-ODS754 is being used in gas turbine engine components, furnace fixtures and skid rails, fasteners and other applications where high temperature creep and corrosion resistance are required [35]. After 1008 h exposure in air with 5 vol.% water vapor at 1450 K, the amount of material lost from the surface of MA-ODS754 was only 2.5 μm (the maximum depth of the attack layer was <96 μm), compared to 43 μm for Inconel 601 under the same conditions [35]. The formation of an alumina protective scale and the high nickel content in MA-ODS754 provide excellent nitration resistance. After 1008 h exposure in N_2–5 vol.%H_2 at 1450 K, surface losses were only 2.4 μm, compared to 8 μm for Inconel 601 [35].

MA-ODS956 was developed for use in aerospace industry. The distribution of fine yttria particles in this highly corrosion resistant alloy results in high creep strength in prolonged high temperature operation above 1100 °C, to even 1300 °C [35]. The high Al content (4.5 wt% nominal) forms a thin, highly adherent and protective surface layer (or scale) of alumina (Al_2O_3), even when levels of oxygen are low. The adhesion of the alumina scale is improved by the mobility of the yttrium in the fine Y_2O_3 oxide dispersoids [53]. Cyclic and isothermal oxidation experiments involving MA-ODS956 have been conducted at 1200 °C in dry, flowing O_2, and the mass gains in test specimens were measured continuously [53]. Each test cycle consisted of 2 h at temperature followed by >5 min cooling to room

temperature. After twenty, 2-h cycle at 1200 °C, the mass gain in MA-ODS956 was 0.85 mg/cm^2, which corresponds to a surface layer that is 1.2 μm thick. The parabolic oxidation rate constants of MA-ODS956 in air are 1.9×10^{-14} and 5.8×10^{-14} g^2/cm^4 s at 900 °C and 1000 °C, respectively, compared to 4.0×10^{-14} and 100×10^{-14} g^2/cm^4 s for MA-ODS754 at the same temperatures [54]. The alumina scale of MA-ODS956 is also a barrier for carburization and sulfidation. It greatly reduces the carbon diffusion rate into the base metal as well as the adherence of carbon deposits onto the alumina surface [35]. Under carburization conditions, a relatively clean surface of this alloy maintains excellent heat transfer rates in radiant heating and chemical processing applications, thus reducing the risk of overheating the alloy. When tested at 1366 K in 2 vol.%CH_4, 93 vol.%H_2, 5 vol.%Ar, the measured weight gain was only 10% of that for Inconel 601 [35] under the same conditions.

3.5. Compatibility of MA-ODS alloys with alkali liquid metals

Generally, there is very little data on compatibility of MA-ODS ferritic steels with Na and Li liquids, and most data are limited to a maximum temperature of ~600 °C. Corrosion tests performed to evaluate the suitability of 9Cr–1Mo MA-ODS steel (88.65 wt%Fe, 9 wt%Cr, 1 wt%Mo, 0.25 wt%V, 0.4 wt%Mn, 0.1 wt%C, 0.5 wt%Si, 0.1 wt%Nb) as a structural material in Japan's high temperature fast reactors showed good compatibility with liquid Na up to 823 K. The measured corrosion rate in the presence of 1-ppm O_2 was <0.2 μm/year, increasing by an order of magnitude to <2 μm/year in 5-ppm O_2 [62]. Compatibility tests of Fe–9Cr and Fe–12Cr ferritic MA-ODS steels with Li and Pb–17Li performed at temperatures up to 600 °C [63,64] showed higher resistance to corrosion than 316-SS, with measured weight loss increasing linearly with time. The linear kinetics suggests that the weight loss is controlled by dissolution of MA-ODS steel constituents, rather than by impurities or solid reaction products. Visual observations indicated preferential depletion of Cr, possibly due to reactions with nitrogen or carbon in the colder parts of the Li loop [63,64]. Test results to date provide strong evidence that the corrosion rate of the MA-ODS steels in Li does not always increase with temperature.

Even though MA-ODS957 steel could be more compatible with Na and Li liquids than MA-ODS754 and MA-ODS956 alloys, compatibility tests at high temperatures up to 1300 K or even higher do not exist and are required. The Al in the amount of 4.5 wt% in MA-ODS956 steel could compromise its compatibility with liquid metals [43,44]. Fischer [49] recommends that if these alloys are to be used in liquid metal-cooled reactors, the Al content should be limited to <1 wt%. Similarly, the high Ni content in MA-ODS754 (78 wt%Ni, 20 wt%Cr, 1 wt%Fe, 0.5 wt%Ti, 0.3 wt%Al, 0.05 wt%C, and 0.6 wt%Y_2O_3) raises a flag about its compatibility with alkali liquid metals, since Ni has been shown to leach out from other Ni-based alloys in the past. For example, measured corrosion rate of Inconel 600 (~77wt%Ni) due to preferential dissolution of nickel in liquid sodium with 10-ppm oxygen at 923 K was 150 μm/year, compared to 20 μm/year for 316-SS (with only 10 wt%Ni) [17].

3.6. Fabricability and weldability of MA ODS alloys

The ODS ferritic alloys have not only the desirable properties attributable to conventional ferritic alloys, but also high-temperature mechanical strength and are readily fabricable at ambient temperature. They are less expensive than refractory alloys; however, MA-ODS957 is not currently produced commercially, but could be fabricated by Special Metals Corporation on a special order. On the other hand both MA-ODS754 and MA-ODS956 are commercially available for a host of high temperature industrial applications.

The Inconel MA754 is one of the most creep-resistant commercially available alloys for service over 1370 K. This characteristic offers superior resistance to bowing and sagging under load at high temperatures. This alloy has good thermal fatigue resistance compared to many high strength superalloys, and is readily machined by all conventional techniques [35]. The strongest joints are produced by several processes, such as laser and electron beam welding [44], and diffusion bonding.

Brazing of MA-ODS754 has been done for years with great success in applications such as gas turbine engines. Mechanical joints such as rivets, pins, threaded connections and fir tree joints are also often used [35]. Conventional tungsten inert-gas (TIG) welding can be used but reduces the high-temperature stress rupture strength at the joint. In the final annealed condition, MA-ODS754 has a coarse, creep resistant grain structure, and thus exhibits limited hot formability. It can be hot worked into the desired shape prior to the grain-coarsening final anneal.

A full range of hot- and cold-worked MA-ODS956 products is available. The forming and machining characteristics of this alloy are similar to those of conventional high-chromium ferritic steels and Fe–Cr–Al alloys [35]. Although it is possible to use high-speed steel tools, it is usually more economical to employ carbide-tipped tools. Cutting with an abrasive saw requires care to avoid thermal shock which can cause cracking; if possible a cooling fluid should be used. If electric discharge machining (EDM) is to be used, the recast surface layer must be subsequently removed by grinding.

Conventional TIG welding of MA-ODS956 is possible but produces relatively low strength joints, which are acceptable for positioning and fillet type welds. Suitable filler wires are Inconel filler metal 82 for dissimilar metal joints, to nickel-base alloys and matching composition wires for welding to austenitic stainless steels. For joining this alloy to itself a Fe–Cr–Al wire is recommended where high-temperature oxidation resistance is required in the weld. The strongest joints are produced by processes of high energy density, such as laser and electron beam welding [44]. If it is impossible to avoid highly restrained joint designs, post-weld stress relieving should be carried out as soon as practicable to avoid delayed stress cracking. A treatment for 2 h at 1100 °C (2010 °F) in air followed by air cooling can be used [35]. The same cycle may serve as a pre-oxidation treatment, provided the surface is cleaned of lubricants and other contaminants. Brazing, diffusion bonding, and transient liquid phase bonding (TLP) are possible if care is taken to first remove the protective alumina film by grinding.

For maximum strength at high temperatures, mechanical joints such as matching composition rivets, pins and threaded connections are often used for MA-ODS956 [35]. The nature of this ferritic alloy requires care in high-strain-rate forming operations such as bending, deep drawing, punching and shearing. For severe deformations it is recommended that the material and the tooling are warmed to 150–200 °C.

The desired microstructure of MA-ODS957 cannot be regenerated once eliminated by re-crystallization during thermal annealing, putting an upper limit on the annealing temperature [37]. The final processing window determined from experiments indicated that both cracking and re-crystallization can be avoided if cold work is held to about 15% or less, and annealing temperatures at around 1273 K. As with MA-ODS956, the oxide dispersion added to strengthen the alloy makes MA-ODS957 a difficult alloy to weld by traditional fusion methods, due to the porosity and slag created during the melting process, and the inherent weakness of the weld metal following removal of the dispersoids [37]. The feasibility of pulse magnetic welding (PMW) has been demonstrated on both MA956 and MA957 tubing, although the optimum weld parameters have not yet been established [37].

4. Summary and conclusions

The mechanical and thermo-physical properties of refractory metal alloys and MA-ODS steels are reviewed and their potential for use in space nuclear reactor power systems is examined. Preferable refractory alloys for use in liquid metal and gas-cooled space reactors include Nb–1%Zr, PWC-11, Mo–TZM, Mo–xRe where x varies from 7% to 44.5%, T-111 and ASTAR-811C. These alloys are heavy, difficult to fabricate, and are not readily available. A key challenge associated with using refractory alloys at present is to re-establish large-scale production capabilities and to recapture former expertise on fabricability, developing viable joints, brazing, cold work in various shapes, irradiation effects, and weldability. While niobium and tantalum alloys are easier to fabricate than molybdenum alloys, they require stringent control of atmospheric impurities (including oxygen and CO_2) and are best handled in glove boxes.

The three MA-ODS alloys investigated in details: Inconel MA-ODS754, Incoloy MA-ODS956, and Incoloy MA-ODS957 offer a number of advantages over refractory alloys in the temperature range between 1000 and 1400 K, namely:

(a) Material strength at high temperatures (>1000 K) is relatively higher and decreases slower with temperature than for niobium (Nb) and molybdenum (Mo) refractory alloys.
(b) The materials are relatively lightweight and less expensive, and have relatively high melting point/re-crystallization temperature and low DBTT, and they retain good strength (>3–4 MPa) up to 75–80% of their melting points.
(c) The materials experience low swelling and embrittlement with exposure to high-energy neutrons (>0.1 MeV) up to a fluence of 10^{27} n/m^2, which is about an order of magnitude higher than expected in space nuclear reactors operating for 7–10 years.
(d) Both MA-ODS754 and MA-ODS956 are produced commercially in large quantities and are used in a host of high temperature industrial applications. MA-ODS956 offers the best combination of high-temperature strength and oxidation resistance. MA-ODS957 has similar characteristics, and although not currently produced commercially, it could be fabricated on a special order.

The few data available on the compatibility of MA-ODS alloys with alkali liquid metals up to 1100 K are encouraging, however, additional tests at typical operating temperatures in space nuclear reactors (1000–1400 K) are needed. The MA-ODS754 alloy has been shown recently to be compatible with liquid sodium at 1223 K for up to 5500 h, however MA-ODS956 does not appear to be compatible with liquid sodium at this temperature, due to its relatively high aluminum content (4.5 wt%). Fabricability of MA-ODS steels may be an issue, but less so than with Mo–Re alloys. For gas-cooled space nuclear reactors at temperatures $\leqslant$1400 K, MA-ODS alloys are particularly very attractive as structure materials. Irradiation tests are needed to verify the compatibility of MA-ODS steels with various types of

nuclear fuel such as UO_2 and UN at typical operation temperatures in space nuclear power systems.

Acknowledgments

This work is funded under NASA grant No. 1249282 to the University of New Mexico's Institute for Space and Nuclear Power Studies. The opinions expressed in this article are solely those of the authors and have neither been endorsed by nor reflect an official position of NASA.

References

[1] S.J. Zinkle, L.J. Ott, D.T. Ingersoll, R.J. Ellis, M.L. Grossbeck, in: M.S. El-Genk (Ed.), Proceedings of Space Technology and Applications International Forum, STAIF-2002, AIP Conference Proceedings No. 608, vol. 1, American Institute of Physics, Melville, NY, 2002, p. 1063.

[2] P.J. Ring, E.D. Sayre, in: M.S. El-Genk (Ed.), Proceedings of Space Technology and Applications International Forum, STAIF-2004, AIP Conference Proceedings No. 699, American Institute of Physics, Melville, NY, 2004, p. 806.

[3] R.E. Mason, M.S. El-Genk, J. Nucl. Mater. 217 (1994) 304.

[4] D.P. Kramer, J.D. Ruhkamp, D.C. McNeil, E.I. Howell, M.K. Williams, J.R. McDougal, R.A. Booher, in: M.S. El-Genk (Ed.), Proceedings of Space Technology and Applications International Forum, STAIF-2000, AIP Conference Proceedings No. 504, vol. 2, American Institute of Physics, New York, NY, 2000, p. 1402.

[5] R.W. Buckman Jr., in: M.S. El-Genk (Ed.), Proceedings of Space Technology and Applications International Forum, STAIF-2004, AIP Conference Proceedings No. 699, American Institute of Physics, Melville, NY, 2004, p. 815.

[6] J.A. Angelo Jr., D. Buden, Space Nuclear Power, Orbit Book, Malabar, FL, 1985, Chapters 9, 11 and 12.

[7] M.S. El-Genk, H. Xue, D. Paramonov, J. Nucl. Technol. 105 (1) (1993) 70.

[8] K.L. Meier, S.P. Girrens, J.M. Dickinson, Proceedings of 15th Intersociety Energy Conversion Engineering Conference, 18–22 August 1980, Seattle, Washington, vol. 1, American Institute of Aeronautics and Astronautics, 1980, p. 762, Paper No. 809144.

[9] K.L. Meier, H.E. Martinez, J.E. Runyan, Proceedings of 16th Intersociety Energy Conversion Engineering Conference, 9–14 August 1981, Atlanta, GA, vol. 1, American Society of Mechanical Engineers, New York, NY, 1981, p. 296, Paper No. 819263.

[10] K.L. Meier, Proceedings of 18th Intersociety Energy Conversion Engineering Conference, 21–26 August 1983, Orlando, FL, vol. 1, Society of Automotive Engineers, 1983, Paper No. 839015.

[11] A.T. Marriott, T. Fujita, in: M.S. El-Genk (Ed.), Proceedings of 11th Symposium on Space Nuclear Power and Propulsion, American Institute of Physics, New York, NY, 1994, p. 157, CONF-940101.

[12] F. Carré, E. Proust, S. Chaudourne, P. Keirle, Z. Tilliette, J.-M. Tournier, B. Vrillon, in: M.S. El-Genk, M.D. Hoover (Eds.), Proceedings of 7th Symposium on Space Nuclear Power and Propulsion, vol. 1, Institute for Space and Nuclear Power Studies, the University of New Mexico, Albuquerque, NM, 1990, p. 381.

[13] M.S. El-Genk, F. Carré, J.-M. Tournier, in: W.D. Jackson (Ed.), Proceedings of 24th Intersociety Energy Conversion Engineering Conference, IEEE, New York, NY, vol. 2 1989, p. 1281, Paper No. 899311.

[14] R.J. Lipinski, R.X. Lenard, S.A. Wright, M.G. Houts, B. Patton, D. Poston, in: M.S. El-Genk (Ed.), Proceedings of the Space Technology and Applications International Forum, STAIF-2000, AIP Conference Proceedings No. 504, American Institute of Physics, New York, NY, 2000, p. 974.

[15] M.S. El-Genk, J.-M. Tournier, Int. J. Progr. Nucl. Energy 45 (1) (2004) 25.

[16] J.R. DiStefano, in: M.S. El-Genk, M.D. Hoover (Eds.), Space Nuclear Power Systems 1988, vol. 9, Orbit Book, Malabar, FL, 1989, p. 299.

[17] J.C. King, M.S. El-Genk, J. Propul. Power 17 (3) (2001) 547.

[18] S.J. Zinkle, F.W. Wiffen, in: M.S. El-Genk (Ed.), Proceedings of Space Technology and Applications International Forum, STAIF-2004, AIP Conference Proceedings No. 699, American Institute of Physics, Melville, NY, 2004, p. 733.

[19] W.D. Klopp, in: M.S. El-Genk, M.D. Hoover (Eds.), Space Nuclear Power Systems 1984, vol. 42, Orbit Book Company, Malabar, FL, 1985, p. 359.

[20] L.D. Lundberg, A Critical Evaluation of molybdenum and its alloys for use in space reactor core heat pipes, Los Alamos Scientific Laboratory's Report No. LA-8685-MS, Los Alamos, NM, January 1981.

[21] T. Leonhardt, J.-C. Carlén, M. Buck, C.R. Brinkman, W. Ren, C.O. Stevens, in: M.S. El-Genk (Ed.), Proceedings of Space Technology and Applications International Forum, STAIF-1999, AIP Conference Proceedings No. 458, vol. 1, American Institute of Physics, New York, NY, 1999, p. 685.

[22] R.S. Reid, M.A. Merrigan, J.T. Sena, in: M.S. El-Genk, M.D. Hoover (Eds.), Proceedings of the 8th Symposium on Space Nuclear Power Systems, vol. 3, American Institute of Physics, New York, NY, 1991, p. 999, CONF-910116.

[23] L.D. Lundberg, in: Proceedings of 6th International Heat Pipe Conference, 25–29 May 1987, Grenoble, France, French Atomic Energy Commission (CEA), 1987 44, Paper No. 1.3.43.

[24] E.E. Hoffman, in: M.S. El-Genk, M.D. Hoover (Eds.), Space Nuclear Power Systems 1984, vol. 41, Orbit Book Company, Malabar, FL, 1985, p. 349.

[25] A.F. Condliff, R.J. Marsh, in: M.S. El-Genk, M.D. Hoover (Eds.), Space Nuclear Power Systems 1984, vol. 26, Orbit Book Company, Malabar, FL, 1987, p. 275.

[26] J.R. Stephens, in: M.S. El-Genk, M.D. Hoover (Eds.), Space Nuclear Power Systems 1986, vol. 28, Orbit Book, Malabar, FL, 1987, p. 291.

[27] W.A. Ranken, Status of High-temperature Heat Pipe Technology, Los Alamos National Laboratory Report No. LA-UR-82-3340, Los Alamos, NM, 1982.
[28] T.E. Tietz, J.W. Wilson, Behavior and Properties of Refractory Metals, Stanford University, Stanford, CA, 1965, p. 28, 377.
[29] S.R. Lampman, T.B. Zorc, in: Chapter on Refractory Metals and Alloys, Metals Handbook, 10th Ed., vol. 2, American Society for Metals (ASM) International, Metals Park, OH, 1990, p. 557.
[30] Rhenium Alloys, Elyria, OH, URL: http://www.rhenium.com; also data in the MatWeb online material properties database, URL: http://www.matls.com, cited July 1999.
[31] J.A. Horak, in: M.S. El-Genk, M.D. Hoover (Eds.), Space Nuclear Power Systems 1985, vol. 16, Orbit Book, Malabar, FL, 1986, p. 97.
[32] J.B. Conway, in: R.H. Cooper Jr., E.E. Hoffman (Eds.), Proceedings of Symposium on Refractory Alloy Technology for Space Nuclear Power Applications, 10–11 August 1983, Oak Ridfe, TN, Technical Information Center, Office of Scientific and Technical Information, US DOE, 1984, p. 227.
[33] D.I. Poston, R.J. Kapernick, R.M. Guffee, in: M.S. El-Genk (Ed.), Proceedings of Space Technology and Applications International Forum, STAIF-2002, AIP Conference Proceedings No. 608, American Institute of Physics, Melville, NY, 2002, p. 578.
[34] J.C. King, M.S. El-Genk, in: M.S. El-Genk (Ed.), AIP Conference Proceedings No. 699, American Institute of Physics, Melville, NY, 2004, p. 319.
[35] Special Metals Corporation, Products and Publications, http://www.specialmetals.com., 2003.
[36] M.L. Hamilton, D.S. Gelles, R.J. Lobsinger, G.D. Johnson, W.F. Brown, M.M. Paxton, R.J. Puigh, C.R. Eiholzer, C. Martinez, M.A. Blotter, Fabrication technological development of the oxide dispersion strengthened alloy MA957 for fast reactor applications, Report No. PNNL-13168, Pacific Northwest Laboratory, Richland, WA, February 2000.
[37] M.L. Hamilton, D.S. Gelles, R.J. Lobsinger, M.M. Paxton, W.F. Brown, Fabrication Technology for ODS Alloy MA957, Report No. PNL-13165, Pacific Northwest Laboratory, Richland, WA, February 2000.
[38] S. Ukai, M. Harada, H. Okada, M. Inoue, S. Nomura, S. Shikakura, K. Asabe, T. Nishida, M. Fujiwara, J. Nucl. Mater. 204 (1993) 65.
[39] R.L. Klueh et al., J. Nucl. Mater. 307–311 (2002) 773.
[40] R. Lindau, A. Moslang, M. Schirra, P. Schlossmacher, M. Klimenkov, J. Nucl. Mater. 307–311 (2002) 769.
[41] M.A. Merrigan, in: M.S. El-Genk, M.D. Hoover (Eds.), Space Nuclear Power Systems 1984, vol. 48, Orbit Book Company, 1985, p. 419.
[42] M.N. Ivanovskii, V.P. Sorokin, I.V. Yagodkin, in: R. Berman, G. Rice (Eds.), The Physical Principles of Heat Pipes, Oxford University, New York, NY, 1982.
[43] R.S. Reid, T.J. Sena, A.L. Martinez, Heat-pipe Development for Advanced Energy Transport concepts, Final Report Covering the Period January 1999 through September 2001, Los Alamos National Laboratory Report No. LA-13949-PR, Los Alamos, NM, October 2002.
[44] R.S. Reid, T.J. Sena, J.P. Nehrbauer, Sodium Compatibility Tests of MA754 and MA956 alloys, Los Alamos National Laboratory Report, Los Alamos, NM, in press.
[45] R.H. Titran, J.R. Stephens, D.W. Petrasek, Refractory Metal Alloys and Composites for Space Nuclear Power Systems, NASA Technical Memorandum No. 101364, 1988.
[46] J. Singh, D.E. Wolfe, in: M.S. El-Genk (Ed.), Proceedings of Space Technology and Applications International Forum, STAIF-2004, AIP Conference Proceedings No. 699, American Institute of Physics, Melville, NY, 2004, p. 733.
[47] J.P. Moore, J.F. King, J.R. DiStafano, E.K. Ohriner, in: M.S. El-Genk (Ed.), Proceedings of Space Technology and Applications International Forum, STAIF-2004, AIP Conference Proceedings No. 608, American Institute of Physics, Melville, NY, 2004, p. 633.
[48] R. Bowman, F. Ritzert, M. Freedman, in: M.S. El-Genk (Ed.), Proceedings of Space Technology and Applications International Forum, STAIF-2004, AIP Conference Proceedings No. 699, American Institute of Physics, Melville, NY, 2004, p. 821.
[49] J.J. Fischer, United States Patent No. 4,075,010, assigned to The International Nickel Company, New York, NY, 21 February 1978.
[50] T. Yoshitake, T. Ohmori, S. Miyakawa, J. Nucl. Mater. 307–311 (2002) 788.
[51] S. Ukai, M. Fujiwara, J. Nucl. Mater. 307–311 (2002) 749.
[52] S. Ukai, T. Nishida, T. Okuda, T. Yoshitake, J. Nucl. Mater. 258–263 (1998) 1745.
[53] B.A. Pint, A.J. Garratt-Reed, L.W. Hobbs, Oxidation Met. 56 (1/2) (2001) 119.
[54] B.A. Pint, I.G. Wright, J. Nucl. Mater. 307–311 (2002) 763.
[55] K. Kurome, S. Date, M. Sukekawa, K. Takakura, N. Kawasaki, Y. Tanaka, in: R. Mohan (Ed.), Advances in Life Prediction Methodology, ASME Pressure Vessels and Piping Conference, PVP-vol. 391, The American Society of Mechanical Engineers, New York, NY, 1999, p. 47.
[56] M. McKimpson, High Performance ODS Tubes for Production of Ethylene and other Industrial Chemicals, Michigan Technological University, Houghton, MI, web site: http://www.imp.mtu.edu/webform/ODS_Tubes_Project.html, 2003.
[57] D.J. Senor, J.K. Thomas, K.L. Peddicord, in: M.S. El-Genk, M.D. Hoover (Eds.), Transactions of the 6th Symposium on Space Nuclear Power Systems, 8–12 January 1989, Albuquerque, NM, ISNPS, the University of New Mexico, Albuquerque, NM, 1989, p. 205, CONF-890103-Summs.
[58] Y.S. Touloukian, E.H. Buyco, in: Thermophysical Properties of Matter, The TPRC Data Series, vol. 4, IFI/Plenum, New York, NY, 1970.
[59] Y.S. Touloukian, R.K. Kirby, R.E. Taylor, P.D. Desai, in: Thermophysical Properties of Matter, the TPRC Data Series, vol. 12, IFI/Plenum, New York, NY, 1975.
[60] V.V. Sagaradze, V.I. Shalaev, V.L. Arbuzov, B.N. Goshchitskii, Y. Tian, W. Qun, S. Jiquang, J. Nucl. Mater. 295 (2001) 265.

[61] D.S. Gelles, J. Nucl. Mater. 233–237 (1996) 293.
[62] T. Asayama, T. Furukawa, E. Yoshida, in: R. Mohan (Ed.), Advances in Life Prediction Methodology, 1999 ASME Pressure Vessels and Piping Conference, PVP-vol. 391, The American Society of Mechanical Engineers, New York, NY, 1999, p. 61.
[63] O.K. Chopra, D.L. Smith, J. Nucl. Mater. 191–194 (1988) 965.
[64] P.F. Tortorelli, J. Nucl. Mater. 155–157 (1992) 715.